

# Curcumin-loaded Polycaprolactone/Collagen Composite Fibers as Potential Antibacterial Wound Dressing

E. San Martín-Martínez<sup>1</sup>, R. Casañas-Pimentel<sup>1</sup>, A. Almaguer-Flores<sup>2</sup>, G. Prado-Prone<sup>2</sup>,  
A. García-García<sup>3</sup>, C. Landa-Solís<sup>4</sup>, and A. Hernández-Rangel<sup>1\*</sup>

<sup>1</sup>Center for Research in Applied Science and Advanced Technology, CICATA-Legaria, National Polytechnic Institute, Legaria 694, Col. Irrigación, CDMX, 11500, México

<sup>2</sup>Faculty of Dentistry, Postdoctoral and Research Division, National Autonomous University of Mexico, Circuito Exterior s/n, Ciudad Universitaria, CDMX, 04510, México

<sup>3</sup>Group of Synthesis and Modification of Nanostructures and Bidimensional Materials. Center for Research in Advanced Materials (CIMAV - Monterrey), PIIT, Apodaca N.L., 66628, Mexico

<sup>4</sup>Tissue Engineering Unit, National Institute of Rehabilitation Luis Guillermo Ibarra Ibarra, Calz México-Xochimilco 289, CDMX, 14389, México

(Received November 25, 2021; Revised February 1, 2022; Accepted February 7, 2022)

**Abstract:** The development of wound dressings with therapeutical benefits is of great importance in skin tissue engineering applications, adding bioactive molecules into biomaterials is a strategy to achieve a better biological response. In this study, four different concentrations of curcumin (CUR; 5, 10, 15 and 20 by weight in relation to the PCL content) were incorporated into solutions composed of polycaprolactone (PCL) and collagen (COL) for the manufacture of electrospun fibers. The PCL-COL-CUR fibers were physicochemically characterized in terms of their morphology, wettability, degradation rate, mechanical behavior, and cumulative curcumin release. The *in vitro* biological properties of the composite membranes were also evaluated. The results indicated that the membranes have diameters on average of approximately 200 nm. The water uptake was adequate for exudates remotion in a wound, and the degradation rate of the fibers was highly appropriate to achieve complete skin tissue regeneration. The addition of CUR to composite membranes produced a significant increase in the mechanical properties which indicate a satisfactory clinical handling. The incorporation of CUR produced a significant decrease in the planktonic growth of *S. aureus* over time, however, the antibacterial effect against *E. coli* was limited, the presence of CUR did not cause the inhibition of its growth. Finally, the viability of human dermal fibroblasts seeded on the top of the membranes indicated the cytotoxic dosage effect of CUR, the two highest CUR concentrations produced a significant loss of cell viability. Overall, our results suggested that the CUR-loaded PCL-COL composite membranes are promising candidates for use as antibacterial dressings to enhance clinical wound management.

**Keywords:** Collagen, Curcumin, Antibacterial, Wound dressing, Electrospinning

## Introduction

Wound dressings are of main importance for the healing process, their principal aim is to act like a temporary cover that aids in the recovery process; however, ensure the optimal conditions for accelerate the heling process requires improving the therapeutic potential of wound dressings [1,2]. The addition of bioactive molecules into biomaterials to create new functional dressings is of great interest. Among bioactive compounds, plant-derived molecules like polyphenols have been used to confer antioxidant and antimicrobial activities to wound dressings [3-5]. Additionally, polyphenols can crosslink natural polymers, in particular collagen and gelatin, which increase their mechanical strength and thermal stability [6,7].

Curcumin is a natural phytochemical polyphenol and is the major active component of turmeric, it is derived from the rhizome of the plant *Curcuma longa* [8,9]. Several studies indicates that curcumin possess antimicrobial [10,11], antioxidant [12,13], anti-tumorigenic [14,15] and

anti-inflammatory properties [16-18]. Curcumin has also been found to increase wound healing through promoting granulation tissue formation, tissue remodeling, and collagen deposition [19]. Curcumin low *in vivo* bioavailability, low solubility in water and rapid degradation hinders its application in wound dressings [20], however, these limitations have led to additional studies aimed at developing suitable vehicles to increase its stability and bioavailability. Nanofibers (NFs) have been considered due to their similarity in size with the microarchitecture of the natural extracellular matrix (ECM). The high surface area of NFs also increases interaction with tissue, which may allow for sustained drug release and also help regulate cell function [21].

Polycaprolactone (PCL) belongs to a group of biodegradable aliphatic polyesters, has good mechanical properties, is not cytotoxic, and is approved by the US Food and Drug Administration (FDA) for human use [22]. As any other aliphatic polyester, PCL is hydrophobic and lack of biologically active functional groups which limits its ability to promote cell adhesion, proliferation and migration [23,24]. These issues can be solved by the addition of a natural polymer like collagen. Collagen is the main constituent

\*Corresponding author: adhernandezra@ipn.mx

of the ECM and therefore the most abundant protein in the human body [25]. Its superior biological properties, compared to other natural or plant-based polymers, make it a perfect choice for tissue engineering applications. Commonly, the principal source of collagen is bovine skin. However, there has been a growing concern about transmissible bovine collagen diseases [26] as well of limited use due to cultural beliefs [27]. Consequently, alternative collagen sources are sought from fish skin or scales, which are by products from the processing of aquatic products [27,28]. More recently, several groups of researchers, have extracted fish collagen from tilapia skin [29-31], demonstrated that it has more similar characteristics to those of collagen extracted from terrestrial animals [32], and have used it successfully in the regeneration of skin tissue. Of the waste products from tilapia processing, its skin is the best source of collagen for tissue-engineering applications [32], particularly because there is no risk of disease transmission to humans.

PCL-collagen composite NFs have been presented to be favorable candidates for skin tissue engineering due to the good mechanical properties, excellent biocompatibility, inexpensive and easy processability [33]. Incorporating collagen into PCL NFs, not only allows to significantly decrease hydrophobicity, but also has a beneficial influence on the cellular response of a material. Collagen works as a signaling substrate for the adhesion, proliferation, and differentiation of endothelial cells growth [31,34]. To the best of our knowledge, curcumin had not been added to this particular blend, however, electrospun fibers had been fabricated from PCL, curcumin and collagen derivative gelatin, the prepared membranes showed great antibacterial performance against methicillin-resistant *Staphylococcus aureus* (MRSA) and extended spectrum  $\beta$  lactamase (ESBL) [35]. Curcumin had also been incorporated into PCL-polyethylene glycol and PCL-polyvinylalcohol to produce electrospun fibers, demonstrating its antibacterial capacity and anti-inflammatory properties [36,37].

Because of the above, in this work, we developed PCL-fish collagen composite NFs loaded with curcumin using acetic acid/water as benign solvent system with the aim to fabricate PCL-COL-CUR biocompatible, mechanically stable membranes with antibacterial properties. The capability of the PCL-COL-CUR membranes to inhibit planktonic bacterial growth against *Staphylococcus aureus* (*S. aureus*) and *Escherichia coli* (*E. coli*) was studied. The ability of the membranes to sustain dermal cell viability was evaluated by seeding of human dermal fibroblast (HDF) on top of the materials.

## Experimental

### Materials

PCL (Mn=80 Kda), curcumin, commercial collagen (from calf skin) and glacial acetic acid were purchased from Sigma Aldrich and used as received. Dulbecco's modified Eagle's

Ham's F12 medium (DMEM) was purchased from Caisson, penicillin/streptomycin 0.25 %, trypsin 0.25 % were acquired from Gibco, and Trypticase soy broth (TSB) was purchased from BDBioxon. *S. aureus* (25923<sup>TM</sup>), *E. coli* (33780<sup>TM</sup>), human dermal fibroblasts (PCS-201-012<sup>TM</sup>) and fetal bovine serum (FBS) were obtained from ATCC<sup>®</sup>. Cell viability was assessed using the live/dead (green/red) calcein-AM/ethidium homodimer fluorescent kit (LIVE/DEAD<sup>®</sup> Viability/Cytotoxicity Kit for mammalian cell; Molecular Probes) from Invitrogen and Hank's Balanced Salt Solution acquired from Gibco.

### Collagen Extraction and Purification

COL was extracted and purified from tilapia skin by acid treatment as reported in previous works [38,39]. The skin was washed and chopped into small pieces, then treated with NaOH 0.1M for 24 h and washed thoroughly with distilled water until neutral pH was achieved. After, the COL extraction was carried out by acetic acid (0.5 M) solubilization at 4 °C for 48 h. The solubilized COL was salted-out with NaCl 7 M and collected by centrifugation, it was then dialyzed against acetic acid 0.1 M and placed in a shaker (Benchmark ScientificIncu-Shaker<sup>TM</sup> 10LR) at 4 °C for 72 h. The dialyzed distilled water was changed every 24 h, followed by deionized water. Finally, the COL isolated was freeze-dried (Labconco FreeZone 4.5) for further use. The obtained COL was compared with a commercial one from calf skin by Fourier-transform infrared (FTIR) spectroscopy (Cary 630, Agilent Technologies).

### Electrospinning Process

The mats were prepared by individually dissolving PCL and COL into acetic acid 90 % v/v, then the COL solution was added to the dissolved PCL to obtain a final concentration of 12 % w/v for PCL and 6 % w/v for COL. In the case of the CUR containing membranes, the CUR was first dispersed in acetic acid 90 % v/v and then added to the previously prepared PCL-COL solution, the final concentrations of CUR were of 5, 10, 15 and 20 % w/w respect to PCL weight. The PCL-COL-CUR solutions were stirred for 24 h and previously to electrospinning, they were sonicated for 10 min. The fibrous materials were fabricated by electrospinning equipment assembled in our laboratory, all the solutions were independently pumped at 0.5 ml h<sup>-1</sup> using a voltage of 15 kV and a distance from tip to collector of 15 cm. A pure PCL membrane was also prepared for comparison. The electrospun membranes were named according to their composition as PCL, PCL-COL, PCL-COL-CUR5, PCL-COL-CUR10, PCL-COL-CUR15 and PCL-COL-CUR20.

### Physicochemical Characterization of Fibers

Morphology of fibrous mats was confirmed by scanning electron microscopy (Fei Nova NanoSEM 200) measurements at 20 kV; the fiber diameter distribution was estimated from

SEM micrographs.

The characteristic bands associated with PCL, COL and CUR were recorded by Fourier-transform infrared (FTIR) spectroscopy using an infrared spectrometer (Cary 630, Agilent Technologies).

The mechanical properties of the prepared materials were measured in a texture machine (TA-XT2i-Texture Analyzer, Texture Technologies Corporation, USA) by a tensile test, the samples were cut with wide 1 cm and height of 3 cm. The test was run at 1.0 mm/h and the stress-strain curves were obtained.

The wettability of the membranes was determined by water uptake capacity. The water uptake capacity was determined by placing the membranes samples (1 cm<sup>2</sup>) in culture wells and incubating in PBS (pH 7.4) at 37 °C. The dry weight of each sample was measured ( $W_1$ ) and after 24 h, the membranes were taken out, water excess was removed with filter paper and membranes were weighed again ( $W_2$ ). The swelling percentage was calculated as  $(W_2 - W_1)/W_1 \times 100$ .

To evaluate the degradation of the membranes, dry samples were weight ( $W_0$ ) and placed in 48-well plates containing complemented culture medium (pH 7.4) at 37 °C, after determined time intervals, the samples were taken out, wash thoroughly with deionized water, left to dry at room temperature and re-weighed ( $W_1$ ). Weight loss percentage was calculated according to  $(W_0 - W_1/W_0) \times 100$ .

Curcumin release from the membranes was determined by placing 15, 7.5, 5.0 and 3.75 mg of PCL-COL-CUR5, PCL-COL-CUR10, PCL-COL-CUR15 and PCL-COL-CUR20, respectively, in complemented culture medium (pH 7.4) at 37 °C for 7 days. At certain time intervals, 1 ml of medium were taken and substitute with fresh medium to maintain a constant volume. The absorption values were then determined by UV-Vis spectrophotometer (Thermo Fisher Scientific Genesys 10S UV-Vis spectrophotometer) at 420 nm. The CUR concentrations were calculated from the calibration curve. Data are presented as cumulative CUR release.

### Antibacterial Performance

The antibacterial activity of the membranes was determined by evaluating the planktonic growth inhibition of *S. aureus* and *E. coli*. Pure cultures of *S. aureus* and *E. coli* were collected from agar plates and resuspended in TSB supplemented with menadione 1 % v/v and hemin 1 % v/v. The bacterial solution was adjusted to an optical density (OD) of 1 at  $\lambda=600$  nm (BioPhotometer D30). Circular sterilized samples (8 mm in diameter) of the membranes were placed in 48-well culture plates in triplicate, individually inoculated with  $1 \times 10^5$  cells ml<sup>-1</sup> and incubated at 37 °C in an orbital shaker incubator (Clever Scientific Ltd.) at 120 rpm. After 1 and 2 days of incubation, the capability of the membranes to inhibit planktonic bacterial growth was estimated by measuring the turbidity of the inoculated

culture media at  $\lambda=595$  nm in a FilterMax F5 multi-mode microplate reader (Molecular Devices, USA). Percent growth inhibition of bacteria exposed to membrane samples was calculated according to % Inhibition =  $100 - [((\text{ODS} - \text{ODS}_1) / (\text{ODB} - \text{OD}_2)) \times 100]$  where ODS=absorbance of supernatants from bacteria incubation with membrane samples, ODS<sub>1</sub>=absorbance of supernatants from membrane incubation with no bacteria, ODB=absorbance of supernatants from bacteria incubation with no membranes and OD<sub>2</sub>=absorbance of culture media only.

### In vitro Cell Culture Studies

Membranes samples (15 mm-diameter) were sterilized by UV light, placed in well plates, and seeded with human dermal fibroblasts (HDF) at 300,000 cells/cm<sup>2</sup>. First, cells were seeded at high density using 50  $\mu$ l cell suspension drops per membrane and samples were incubated for 2 h at 37 °C and 5 % CO<sub>2</sub> to enhance cell attachment on membranes. Then, culture medium was added in excess and samples were placed back in the incubator. Cell viability on films was assessed at 72 h of culture. At this time, independent cell-cultured membranes samples were collected and incubated with ethidium homodimer-1 and calcein-AM in Hank's Balanced Salt Solution, according to the kit manufacturer guidelines, at 37 °C in 5 % CO<sub>2</sub>. Then, samples were rinsed twice with PBS and immediately visualized by Optical/Fluorescence Microscopy (Axio Observer, Carl Zeiss). Images were processed using the AxioVision<sup>®</sup> software.

### Statistical Analysis

Data were analyzed using the analysis of variance (one way ANOVA) followed by Tukey's test for multiple comparisons. All statistical analyses were performed using the software GraphPad PRISM v7.0.

## Results and Discussion

### Collagen Extraction

The FTIR spectra of the extracted collagen (EC) was compared with a commercial calf skin collagen (CC, Figure 1), both spectra show the typical absorption bands of type I collagen. These include the main bands associated to amide regions: amide A (3280-3300 cm<sup>-1</sup>), amide B (2950-2919 cm<sup>-1</sup>), amide I (1600-1700 cm<sup>-1</sup>), amide II (1500-1600 cm<sup>-1</sup>) and amide III (1200-1300 cm<sup>-1</sup>) [39]. The only difference is the lower intensity of the absorption band of amide III for CC in comparison with EC. This band is related to N-H bending and C-N stretching and is involved with the triple helical structure of collagen [40]; different extraction methods held in different extents this structure. Generally, the acid extraction method preserves the collagen triple helix in a major extent [41]; whereas other methods might produce slight changes in the collagen structure due to the loss of N- and C-terminal domains. Based on these

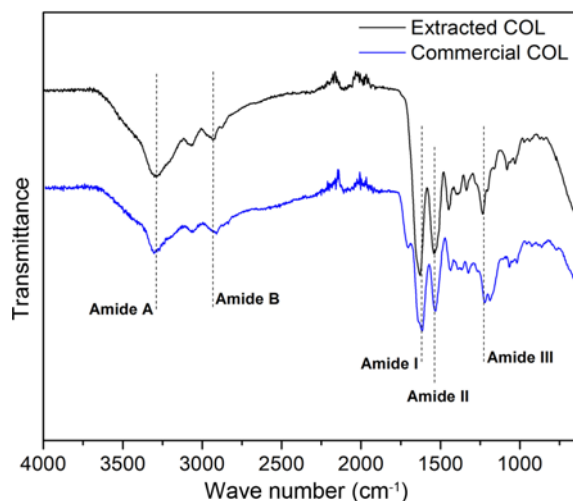


**Figure 1.** FTIR spectra of the acid extracted collagen from tilapia skin and commercial calf skin collagen.

results, it was possible to confirm the successful extraction of collagen type I by acid extraction.

### Physicochemical Characterization of PCL-COL-CUR Membranes

PCL-COL membranes loaded with CUR were fabricated using acetic acid/water as solvent system. PCL-COL fibers by electrospinning technique had been obtained with commonly used hexafluoroisopropanol (HFIP), a highly toxic solvent. As an alternative to HFIP, acetic acid and formic acid had been proposed as a green alternative to produce PCL-COL electrospun membranes [23,42]. Therefore, in this work acetic acid 90 % v/v was selected for fibers fabrication. The morphology of the prepared PCL-COL and PCL-COL-CUR is shown in Figure 2, the fibers displayed uniform structure without bead defects. The CUR incorporation resulted in a slightly decrease of fiber diameters and narrower distribution (Figure 2). However, only a small reduction on fiber diameter was observed, ranging from 218 nm to 200 nm for the PCL-COL and PCL-COL-CUR20, respectively. This higher homogeneity may be attributed to both collagen and curcumin, collagen behavior is polyelectrolyte type which increase the conductivity of polymer solution [28], moreover, enhancement in the spinning solution conductivity due to CUR had also been reported [43].

FTIR spectra (Figure 3A) displays the characteristics bands of PCL at 2942 and 2863  $\text{cm}^{-1}$  ( $\text{CH}_2$  vibrations), the sharp band at 1729  $\text{cm}^{-1}$  due to  $\text{C}=\text{O}$  vibrations, 1470, 1415 and 1365 ( $\text{CH}_2$  bending vibrations),  $\text{COO}$  vibrations at 1238 and 1183  $\text{cm}^{-1}$  and  $\text{C}-\text{O}$  vibrations at 1047 and 1109  $\text{cm}^{-1}$  [44]. For the COL alone the characteristics bands at 3287, 2931, 1632, 1533, 1387, 1450 and 1234  $\text{cm}^{-1}$  for the  $\text{NH}$  stretching vibrations,  $\text{CH}_2$  vibrations,  $\text{C}=\text{O}$  vibrations of amide linkages,  $-\text{NH}$  bending vibrations,  $\text{CH}_2$  bending

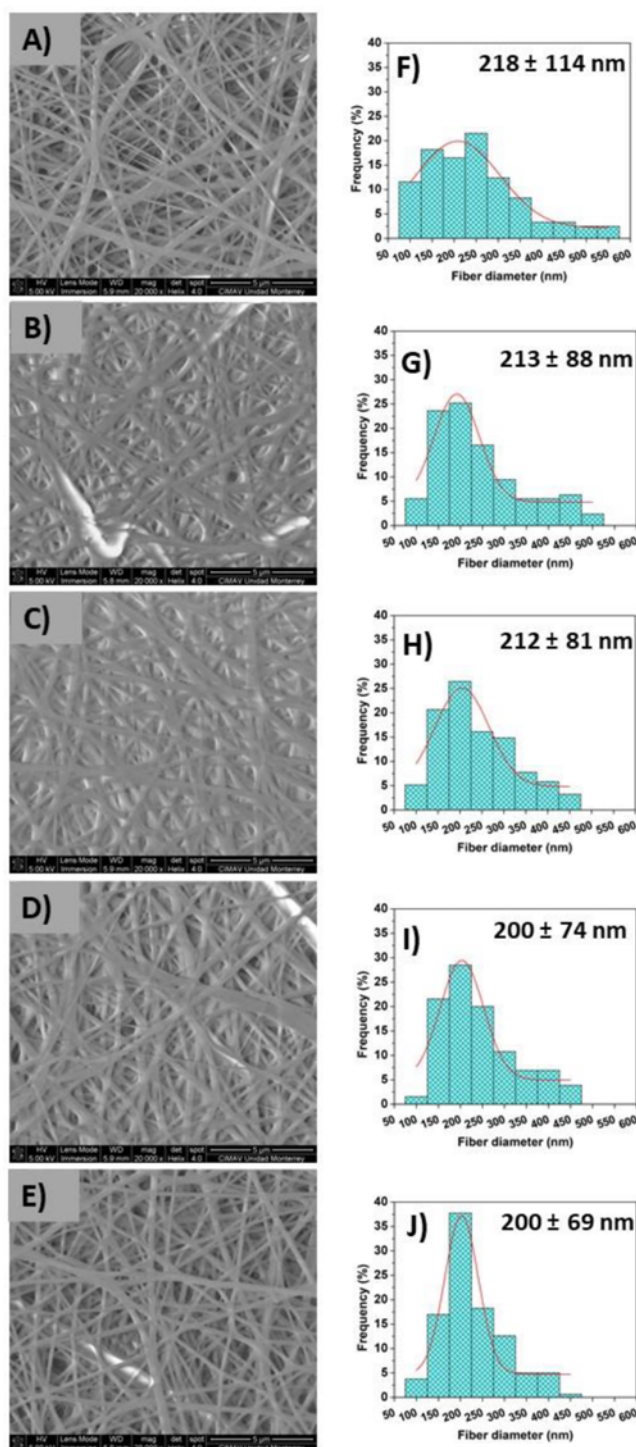


**Figure 2.** Representative SEM micrographs and nanofibers size distribution of PCL-COL (A and F), PCL-COL-CUR5 (B and G), PCL-COL-CUR10 (C and H), PCL-COL-CUR15 (D and I) and PCL-COL-CUR20 (E and J).

vibrations and  $\text{C}-\text{N}$  vibrations are observed, respectively [29]. With respect to the PCL-COL blend, the broad peak

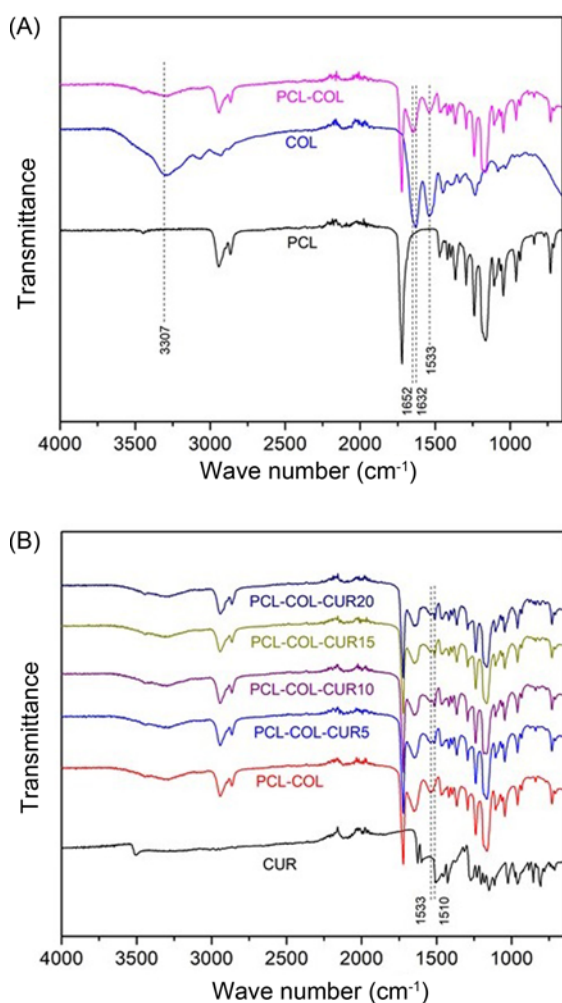


**Figure 3.** FTIR spectrum of composite membranes including (A) pristine PCL membrane, pristine COL and composite PCL-COL membranes and (B) pristine CUR and PCL-COL-CUR membranes.

observed at 3304 cm<sup>-1</sup> might be due to the hydrogen bonding interaction of collagen with PCL. The C=O vibrations of the blend observed at 1633 cm<sup>-1</sup> was about 20 cm<sup>-1</sup> lower than COL alone and suggests that the COL fibers are well dispersed and as a result, nitrogen lone pair of amide link might be highly delocalized over the adjacent C=O group. This delocalization might be the cause for the shift of C=O vibrations to low value. For curcumin (Figure 3B), the bands observed at 3505 cm<sup>-1</sup> (phenolic O-H stretching), 1627 cm<sup>-1</sup> (C=O stretching), 1598 cm<sup>-1</sup> (benzene ring stretching), 1510 cm<sup>-1</sup> (C=C vibrations), 1273 cm<sup>-1</sup> (C-O stretching), and 1145 cm<sup>-1</sup> (C-O-C stretching modes) [8]. The presence of the peak at 1653 cm<sup>-1</sup> in the PCL-COL-CUR spectra indicated that there was no change in the alpha helical conformation of collagen [46], however, the corresponding peak to the triple helix form of collagen (1533 cm<sup>-1</sup>, amide II bands) losses intensity with curcumin incorporation and the corresponding

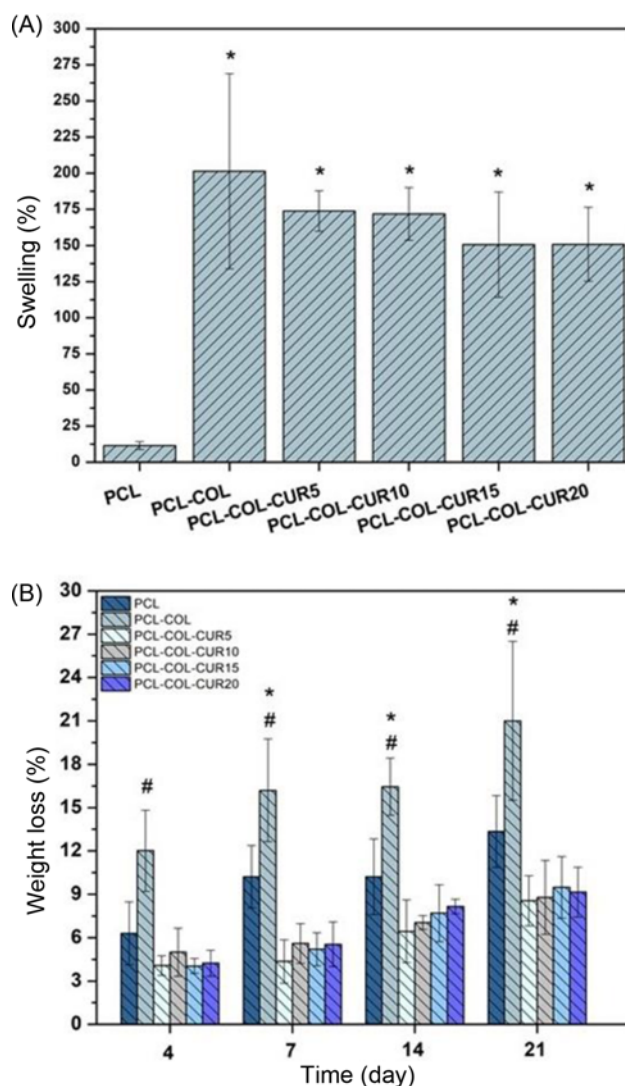


**Figure 4.** (A) Analysis of water uptake capacity by swelling percentage of pristine PCL, PCL-COL and PCL-COL-CUR membranes incubated in PBS at 37 °C. (B) Weight loss percentage over time of pristine PCL, PCL-COL and PCL-COL-CUR membranes incubated in culture medium at 37 °C. Statistical significance is indicated as \* $p < 0.005$  respect to PCL and # $p < 0.005$  respect to PCL-COL.

band for C=C vibrations of curcumin (1510 cm<sup>-1</sup>) appeared in the composite membranes spectra (Figure 3B). Changes in amide II peak might implied that the secondary structure of collagen is lost [46], nonetheless, research findings demonstrated that curcumin does not alter the structural behavior of collagen [47,48], rather, it contributes to collagen stabilization. At acidic pH, curcumin is positively charged which enable its interaction with the negative charges of collagen [47], therefore, a crosslinking effect is formed, increasing the stability and viscosity of collagen.

The hydrophilicity of the membranes was evaluated by



swelling capacity. Swelling is an important parameter as it can simulate body fluid uptake and nutrient penetration within scaffolds structure. Figure 4A clearly shows that COL produced a significant increase in water uptake capacity from only 11 % for p-PCL to 201 % for PCL-COL membrane; there was a total change from hydrophobic to hydrophilic material with COL addition into PCL. As PCL, CUR presents hydrophobic nature, however, its incorporation into the materials did not significantly influence the water uptake properties of composite membranes. The water uptake capacity of PCL-COL-CUR membranes is then adequate for the uptake of wound fluid, which results in early wound closure and healing. Moreover, it has been reported that the wettability of a material controls cell attachment, proliferation and spreading [49]. The greater the hydrophilicity of the surface, the higher the cell growth and proliferation. The higher water uptake capacity of PCL-COL-CUR membranes indicates superior tissue regeneration properties compared to pristine PCL.

The percentage of weight loss for the composite membranes is presented in Figure 4B, the membranes degradation increased with incubation time (4, 7, 14 and 21 days). It is noted that degradation rate is dependent on materials composition, PCL-COL showed the higher degradation rate, at 21 days, the weight loss percentage was of 21 %, i.e., it degrades a 60 % faster than p-PCL membrane. Interestingly, CUR addition produced a slower degradation rate in comparison to PCL-COL membrane, we hypothesized that CUR prevents the rapid solubilization of COL into media by the strong interaction with amide II group as evidenced in FTIR results. For all the CUR compositions, the weight loss percentage varied from around 5 % to approximately 9 %, at 4 and 21 days, respectively, similar data were obtained for p-PCL. The results suggest that the CUR loaded membranes have enhanced stability compared to PCL-COL membranes; wounded skin requires of around 21 days to recover, therefore the developed fibers are expected to support wound healing by allowing cell proliferation and ECM production [44].

Figure 5A shows the representative stress-strain curves of PCL-COL and PCL-COL-CUR membranes and in Table 1 the modulus, elongation at break and maximum tensile strength of the fibers are summarized. The results indicated

that the mechanical properties were improved by the addition of CUR, the membranes with the highest amount of CUR (15 and 20 %) showed a tensile strength value three times higher than that of PCL-COL while the CUR5 and CUR20 membranes improved their tensile strength by 1.5 times respect to PCL-COL. Improvement on mechanical

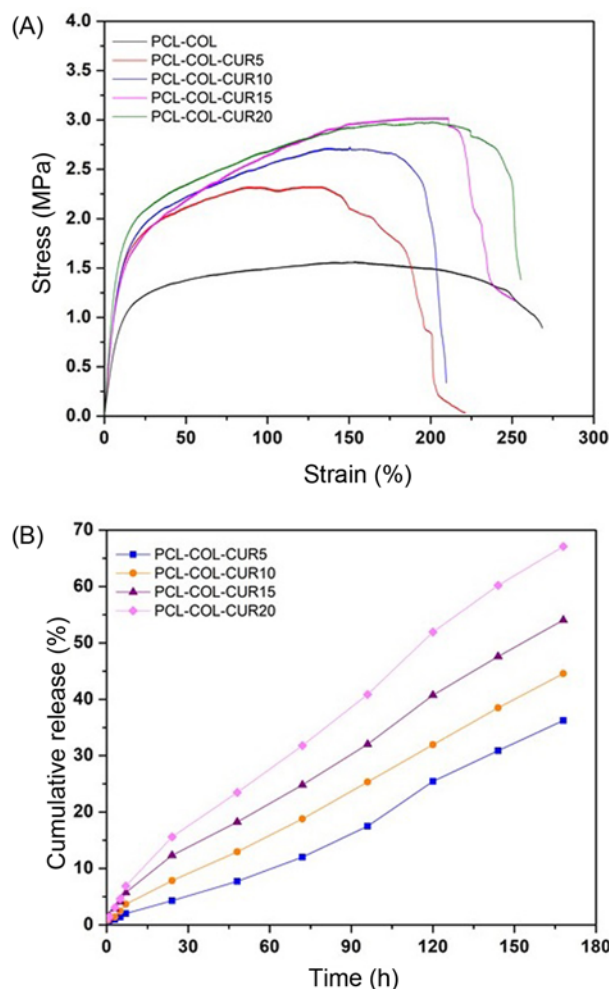


**Figure 5.** (A) Representative stress-strain curves of PCL-COL and PCL-COL-CUR membranes. (B) Cumulative curcumin released from PCL-COL-CUR composite membranes after 180 h of incubation in culture medium at 37 °C and pH 7.4.

**Table 1.** Mechanical parameters calculated from the strain-stress curves of the membranes

Membrane	Elastic modulus (MPa)	Maximum tensile strength (MPa)	Elongation at break (%)
PCL-COL	0.073±0.012	1.55±0.038	218.75±9.01
PCL-COL-CUR5	0.128±0.007*	2.33±0.033*	145.00±5.71*
PCL-COL-CUR10	0.134±0.011*	2.70±0.168*	173.75±6.24*
PCL-COL-CUR15	0.158±0.011*	2.81±0.190*	197.25±8.42*
PCL-COL-CUR20	0.167±0.005*	2.85±0.085*	205.75±8.09

\*Statistical significance  $p < 0.005$  respect to PCL-COL.

performance due to CUR was also found by Mohammadi and Bahrami [50] when CUR (1 to 3 wt%) was added to PCL/gum tragacanth electrospun membranes. The good mechanical stability observed when CUR is added may be attributed to the ambient interaction of collagen with CUR leading to more hydrogen linkages in the triple helix and resulting in higher tensile strength. The presence of two keto groups and one hydroxyl group of curcumin may interact with the side chain moieties of amino acids to produce a type of crosslinking of COL [46]. Mechanical data on electrospun fibrous scaffold for tissue engineering are limited. However, tensile strength of electrospun fibrous mats ranging from 0.8 to 18.0 MPa was found to be sufficiently durable for dermal cell culture [51,52].

In order to analyze the therapeutic activity of the obtained PCL-COL-CUR membranes as a drug delivery system, the *in vitro* cumulative CUR release was studied in physiological conditions (pH 7.4 and 37 °C). Due to the low solubility of CUR in water, its bioavailability in infectious sites is a major issue in the case of CUR loaded drug delivery systems [20]. Therefore, in this study the delivery system was complemented culture medium to simulate the normal body conditions, without the addition of components that promote CUR release like ethanol or tween 80. The release characteristics of CUR from PCL-COL-CUR electrospun mats are shown in Figure 5B, at 168 h (7 days), the composite membranes showed a release of 36, 44, 54 and 67 % for PCL-COL-CUR5, PCL-COL-CUR10, PCL-COL-CUR15 and PCL-COL-CUR20, respectively. It can be noted that the CUR release is gradually increasing with time for all cases, the membranes did not show a burst release, frequently this behavior is observed during the first 8 to 24 hours, in this study the cumulative CUR release after 24 hours for PCL-COL-CUR5, PCL-COL-CUR10, PCL-COL-CUR15 and PCL-COL-CUR20 was of 4.2, 7.8, 12.3 and 15.6 %, respectively. For all cases, the releasing seems to be linear with time, at 7 days there was no plateau behavior, indicating that the developed membranes sustain a continuous CUR releasing over time. The latter might be effect of COL incorporation to composite membranes, in another study it was probed that PCL/CUR system produced a high amount of burst release and a limited CUR releasing, however, when gum tragacanth polysaccharide was included in the membranes a relatively sustained CUR release was achieved [50]. It should also be noted that CUR slow release to the release medium will increase its bioavailability [53]. In fact, the antibacterial results given in the next section support this.

### Antibacterial Activity

Antibacterial performance was analyzed against Gram-negative *E. coli* and Gram-positive bacteria *S. aureus*, Figure 6 displays the percentage of bacterial growth inhibition. As observed from Figure 6A, the antibacterial action against *S. aureus* was related with CUR concentration, as it increases

so does the percentage of inhibition. For control membrane (PCL-COL) and the lowest CUR dosage probed, it can be seen similar behavior, the bacterial inhibition was of 40 % at 24 hours of culture and it remains the same with time (72 hours). In the case of PCL-COL-CUR10, -CUR15 and -CUR20, the inhibition at 24 hours was of 45, 52 and 62 %, respectively. After 72 hours of incubation, a significant improvement in antibacterial action was observed with bacterial inhibition of 65, 67 and 82 %, being -CUR20 the most effective material against *S. aureus*. On the other hand, the materials showed reduced action when tested with *E. coli* (Figure 6B), independently if CUR was present on the materials and its amount, the inhibition percentage was similar at 24 hours of culture (40 %) for all membranes, after 72 hours, only the highest amount of CUR tested sustain the

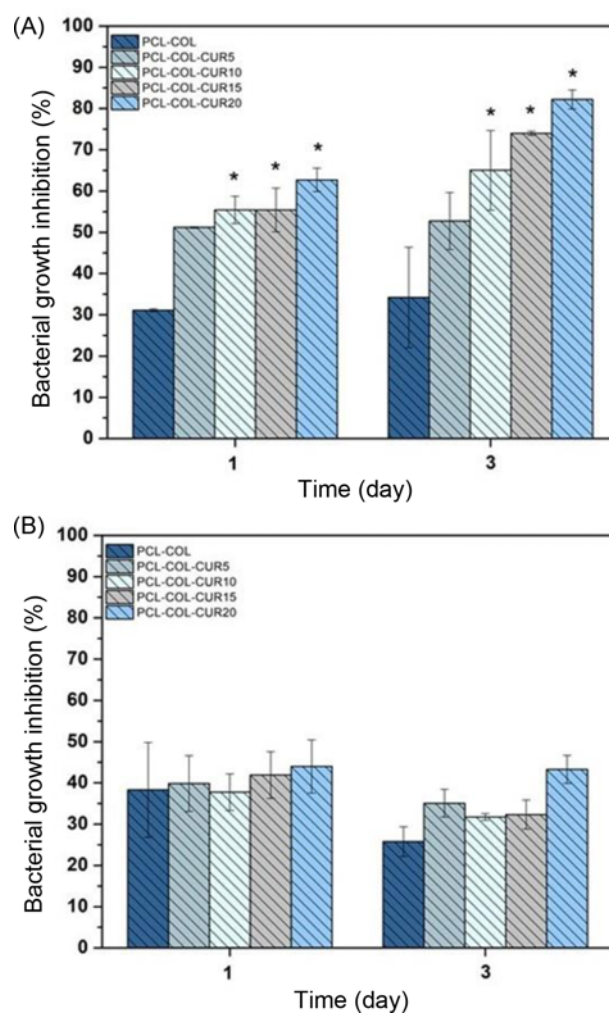


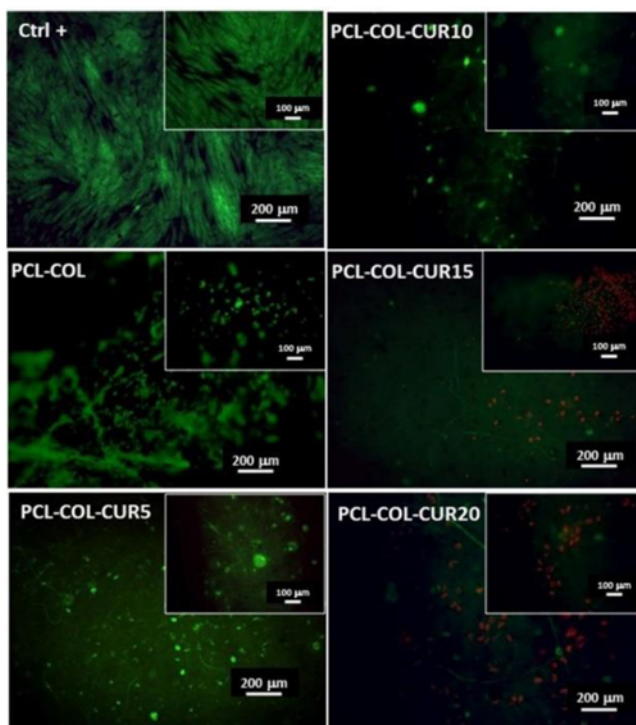
**Figure 6.** Bacterial growth inhibition of (A) *S. aureus* and (B) *E. coli* in the presence of PCL-COL and PCL-COL-CUR membranes measured by the turbidity assay after 1 and 3 days of culture. Statistical significance is indicated as \* $p < 0.005$  respect to PCL-COL.

40 % of inhibition, the remain fibers showed a reduction (35 %) on the inhibition percentage, i.e., they were less effective for hinder the proliferation of *E. coli*. Our results are in agreement with previous studies, CUR superior antibacterial action against Gram-positive bacteria had been

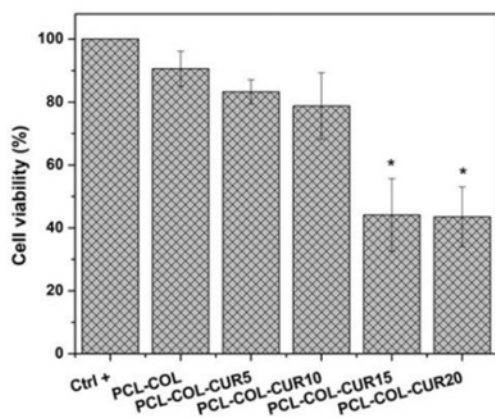
found in comparison to Gram-negative bacteria [54-56]. The latter could be result of the differences in the bacterial cell walls. Gram-positive bacteria contain an outer peptidoglycan layer, while Gram-negative bacteria contain an outer phospholipid membrane, therefore, different types of interactions with CUR are expected [57,58].

### In vitro Biocompatibility of the Membranes

To investigate the biocompatibility of the membranes, calcein AM/ethidium homodimer assay at 72 h of culture was performed to assess cell viability. Representative images and statistical analysis of cell viability percentage are shown in Figure 7 (number of viable cells over total number of cells on each membrane). Results confirmed that cytotoxicity was CUR concentration dependent. HDFs were viable on PCL-COL, PCL-COL-CUR5 and PCL-COL-CUR10 membranes as evidenced by the green calcein fluorescence, with viability percentage of 90, 83 and 80 %, respectively. However, a significant reduction on HDFs viability was noted for PCL-COL-CUR15 and PCL-COL-CUR10 fibers (less than 40 % of cell viability). Increasing CUR concentration and cytotoxic effects towards fibroblasts cells was also reported by other authors [50,54,59]. In another study a significant decrease in endothelial cell adhesion was observed in COL aerogels crosslinked with CUR [46]. Nonetheless, the encapsulation of CUR into nanofibers can overcome CUR side effects by the sustain release at low dosage, being PCL-COL-CUR5 and PCL-COL-CUR10 membranes suitable for dermal exposure.



(A)



(B)

**Figure 7.** (A) Cell viability (Live/Dead, calcein AM/ethidium bromide, assays) of human dermal fibroblasts cultured on PCL-COL and PCL-COL-CUR membranes at 3 days of culture. Viable and dead cells are observed in green and red, respectively. (B) Quantitative analysis of cell viability in percentage (number of viable cells over total number of cells on the membrane) at 3 days of culture; statistical significance is indicated as \* $p < 0.005$  respect to PCL-COL.

### Conclusion

Curcumin loaded PCL/collagen nanofibrous membranes were successfully developed by electrospinning technique. The obtained nanofibers demonstrated the essential physico-chemical properties required for wound dressing applications. SEM results confirmed the formation of bead-free fibers with diameter sizes around 200 nm. Water uptake studies revealed that the PCL-COL-CUR formulations are capable of retain the adequate moisture. The degradation rate and mechanical properties of the membranes were improved by CUR incorporation, probably due to a crosslinking effect of collagen by CUR. *In vitro* drug release studies have demonstrated the sustained CUR release during a long period of time and no burst release effect was observed. Furthermore, the planktonic growth inhibition results confirmed the bactericidal action of CUR against *S. aureus*, however, the membranes did not have a significant effect when tested against *E. coli*. The biocompatibility test showed that HDF viability was CUR dosage dependent, however, with antibacterial results, the PCL-COL-CUR10 membrane sustain antibacterial activity as well of HDF viability and could be a good candidate for wound dressing applications.



## Acknowledgments

A. Hernández Rangel gratefully acknowledges the post-doctoral fellowship provided by the CONACyT México.

## Conflict of Interest

The authors declare no conflict of interest.

## References

1. A. Krishnan and S. Thomas, *Polym. Adv. Technol.*, **30**, 823 (2019).
2. M. Hajialyani, D. Tewari, E. Sobarzo-Sánchez, S. M. Nabavi, M. H. Farzaei, and M. Abdollahi, *Int. J. Nanomedicine*, **13**, 5023 (2018).
3. A. Gaspar-Pintiliescu, A. M. Stanciuc, and O. Craciunescu, *Int. J. Biol. Macromol.*, **138**, 854 (2019).
4. X. Gao, Z. Xu, G. Liu, and J. Wu, *Acta Biomater.*, **119**, 57 (2021).
5. I. Guimarães, S. Baptista-Silva, M. Pintado, and A. L. Oliveira, *Appl. Sci.*, **11**, 1230 (2021).
6. Y. Zhao and Z. Sun, *Int. J. Food Prop.*, **20**, S2822 (2018).
7. R. R. Reddy, B. V. N. Phani Kumar, G. Shanmugam, B. Madhan, and A. B. Mandal, *J. Phys. Chem. B*, **119**, 14076 (2015).
8. M. M. Mahmud, S. Zaman, A. Perveen, R. A. Jahan, M. F. Islam, and M. T. Arafat, *J. Drug Deliv. Sci. Technol.*, **55**, 101386 (2020).
9. N. Ahangari, S. Kargozar, M. Ghayour-Mobarhan, F. Baines, A. Pasdar, A. Sahebkar, G. A. A. Ferns, H. W. Kim, and M. Mozafari, *BioFactors*, **45**, 135 (2019).
10. J. K. Trigo-Gutiérrez, Y. Vega-Chacón, A. B. Soares, and E. G. de O. Mima, *Int. J. Mol. Sci.*, **22**, 7130 (2021).
11. M. Ilangoan, V. Guna, C. Hu, G. S. Nagananda, and N. Reddy, *Ind. Crops Prod.*, **112**, 556 (2018).
12. Y. Fan, J. Yi, Y. Zhang, and W. Yokoyama, *Food Chem.*, **239**, 1210 (2018).
13. R. Meng, Z. Wu, Q. T. Xie, J. S. Cheng, and B. Zhang, *Food Chem.*, **340**, 127893 (2021).
14. I. Nakamae, T. Morimoto, H. Shima, M. Shionyu, H. Fujiki, N. Yoneda-Kato, T. Yokoyama, S. Kanaya, K. Kakiuchi, T. Shirai, E. Meiyanto, and J. Y. Kato, *Molecules*, **24**, 1 (2019).
15. Y. A. Larasati, N. Yoneda-Kato, I. Nakamae, T. Yokoyama, E. Meiyanto, and J. Y. Kato, *Sci. Rep.*, **8**, 1 (2018).
16. N. Fereydouni, M. Darroudi, J. Movaffagh, A. Shahroodi, A. E. Butler, S. Ganjali, and A. Sahebkar, *J. Cell. Physiol.*, **234**, 5537 (2019).
17. E. Blanco-García, F. J. Otero-Espinar, J. Blanco-Méndez, J. M. Leiro-Vidal, and A. Lizardo-Álvarez, *Int. J. Pharm.*, **518**, 86 (2017).
18. T. Esatbeyoglu, K. Ulbrich, C. Rehberg, S. Rohn, and G. Rimbach, *Food Funct.*, **6**, 887 (2015).
19. B. Joe, M. Vijaykumar, and B. R. Lokesh, *Crit. Rev. Food Sci. Nutr.*, **44**, 97 (2004).
20. R. CR, S. PS, O. Manaf, S. PP, and A. Sujith, *Int. J. Biol. Macromol.*, **108**, 1261 (2018).
21. I. Sebe, P. Szabó, B. Kállai-Szabó, and R. Zelkó, *Int. J. Pharm.*, **494**, 516 (2015).
22. S. M. Espinoza, H. I. Patil, E. San Martín Martínez, R. Casañas Pimentel, and P. P. Ige, *Int. J. Polym. Mater. Polym. Biomater.*, **69**, 85 (2020).
23. J. Dulnik, D. Kołbuk, P. Denis, and P. Sajkiewicz, *Eur. Polym. J.*, **104**, 147 (2018).
24. S. R. Gomes, G. Rodrigues, G. G. Martins, M. A. Roberto, M. Mafra, C. M. R. Henriques, and J. C. Silva, *Mater. Sci. Eng. C*, **46**, 348 (2015).
25. A. Hernández-Rangel and E. S. Martín-Martínez, *J. Biomed. Mater. Res. Part A*, **109**, 1751 (2021).
26. E. J. Chong, T. T. Phan, I. J. Lim, Y. Z. Zhang, B. H. Bay, S. Ramakrishna, and C. T. Lim, *Acta Biomater.*, **3**, 321 (2007).
27. K. S. Silvipriya, K. Krishna Kumar, B. Dinesh Kumar, A. John, and P. Lakshmanan, *Curr. Trends Biotechnol. Pharm.*, **10**, 374 (2016).
28. Q. Zhang, S. Lv, J. Lu, S. Jiang, and L. Lin, *Int. J. Biol. Macromol.*, **76**, 94 (2015).
29. C. Bi, X. Li, Q. Xin, W. Han, C. Shi, R. Guo, W. Shi, R. Qiao, X. Wang, and J. Zhong, *J. Biosci. Bioeng.*, **128**, 234 (2019).
30. Q. Li, L. Mu, F. Zhang, Y. Sun, Q. Chen, C. Xie, and H. Wang, *Mater. Sci. Eng. C*, **80**, 346 (2017).
31. T. Zhou, N. Wang, Y. Xue, T. Ding, X. Liu, X. Mo, and J. Sun, *Colloids Surfaces B Biointerfaces*, **143**, 415 (2016).
32. A. Afifah, O. Suparno, L. Haditjaroko, and K. Tarman, *IOP Conf. Ser. Earth Environ. Sci.*, **335**, 012031 (2019).
33. M. Ghorbani, P. Nezhad-Mokhtari, and S. Ramazani, *Int. J. Biol. Macromol.*, **153**, 921 (2020).
34. Y. E. Aguirre-Chagala, V. Altuzar, E. León-Sarabia, J. C. Tinoco-Magaña, J. M. Yañez-Limón, and C. Mendoza-Barrera, *Mater. Sci. Eng. C*, **76**, 897 (2017).
35. M. Fallah, S. H. Bahrami, and M. Ranjbar-Mohammadi, *J. Ind. Text.*, **46**, 562 (2016).
36. H. T. Bui, O. H. Chung, J. Dela Cruz, and J. S. Park, *Macromol. Res.*, **22**, 1288 (2014).
37. S. M. Saeed, H. Mirzadeh, M. Zandi, and J. Barzin, *Prog. Biomater.*, **6**, 39 (2017).
38. P. Kittiphattanabawon, S. Benjakul, W. Visessanguan, T. Nagai, and M. Tanaka, *Food Chem.*, **89**, 363 (2005).
39. D. Liu, L. Liang, J. M. Regenstein, and P. Zhou, *Food Chem.*, **133**, 1441 (2012).
40. M. Ahmad and S. Benjakul, *Food Chem.*, **120**, 817 (2010).
41. M. S. Heu, J. H. Lee, H. J. Kim, S. J. Jee, J. S. Lee, Y.-J. Jeon, F. Shahidi, and J.-S. Kim, *Food Sci. Biotechnol.*, **19**, 27 (2010).
42. G. Prado-Prone, P. Silva-Bermudez, M. Bazzar, M. L. Focarete, S. E. Rodil, X. Vidal-Gutiérrez, J. A. García-

- Macedo, V. I. García-Pérez, C. Velasquillo, and A. Almaguer-Flores, *Biomed. Mater.*, **15**, 035006 (2020).
43. X. Z. Sun, G. R. Williams, X. X. Hou, and L. M. Zhu, *Carbohydr. Polym.*, **94**, 147 (2013).
44. M. Zahiri, M. Khanmohammadi, A. Goodarzi, S. Ababzadeh, M. Sagharjoghi Farahani, S. Mohandesnezhad, N. Bahrami, I. Nabipour, and J. Ai, *Int. J. Biol. Macromol.*, **153**, 1241 (2020).
45. C. Bi, X. Li, Q. Xin, W. Han, C. Shi, R. Guo, W. Shi, R. Qiao, X. Wang, and J. Zhong, *J. Biosci. Bioeng.*, **128**, 234 (2019).
46. G. Dharunya, N. Duraipandy, R. Lakra, P. S. Korapatti, R. Jayavel, and M. S. Kiran, *Biomed. Mater.*, **11**, 045011 (2016).
47. N. N. Fathima, R. S. Devi, K. B. Rekha, and A. Dhathathreyan, *J. Chem. Sci.*, **121**, 509 (2009).
48. M. E. Plonska-Brzezinska, D. M. Bobrowska, A. Sharma, P. Rodziewicz, M. Tomczyk, J. Czyrko, and K. Brzezinski, *RSC Adv.*, **5**, 95443 (2015).
49. Y. Arima and H. Iwata, *Biomaterials*, **28**, 3074 (2007).
50. M. Ranjbar-Mohammadi and S. H. Bahrami, *Int. J. Biol. Macromol.*, **84**, 448 (2016).
51. W. Cui, X. Zhu, Y. Yang, X. Li, and Y. Jin, *Mater. Sci. Eng. C*, **29**, 1869 (2009).
52. Y. Yang, X. Zhu, W. Cui, X. Li, and Y. Jin, *Macromol. Mater. Eng.*, **294**, 611 (2009).
53. Y. E. Bulbul, M. Okur, F. Demirtas-Korkmaz, and N. Dilsiz, *Appl. Clay Sci.*, **186**, 105430 (2020).
54. A. Shababdoust, M. Zandi, M. Ehsani, P. Shokrollahi, and R. Foudazi, *Int. J. Pharm.*, **575**, 118947 (2020).
55. A. Sadeghianmaryan, Z. Yazdanpanah, Y. A. Soltani, H. A. Sardroud, M. H. Nasirtabrizi, and X. Chen, *J. Biomater. Sci. Polym. Ed.*, **31**, 169 (2020).
56. G. I. Fakhrollina, F. S. Akhatova, Y. M. Lvov, and R. F. Fakhrollin, *Environ. Sci. Nano*, **2**, 54 (2015).
57. Bhawana, R. K. Basniwal, H. S. Buttar, V. K. Jain, and N. Jain, *J. Agric. Food Chem.*, **59**, 2056 (2011).
58. D. Zheng, C. Huang, H. Huang, Y. Zhao, M. R. U. Khan, H. Zhao, and L. Huang, *Chem. Biodivers.*, **17**, e2000171 (2020).
59. M. Saadipour, A. Karkhaneh, and M. Haghbin Nazarpak, *Int. J. Polym. Mater. Polym. Biomater.*, **71**, 386 (2022).